

Low Redshift Observational Constraints on Dark Energy Models using ANN - CosmicANNEstimator

Ashly Joseph¹, Albin Joseph^{2*}, Christina Terese Joseph¹,
John Paul Martin¹, Sunil Kumar PV³, Sarthak Giri¹

¹Department of Computer Science, IIITKottayam, Kerala, 686635, India.

²Department of Physics, Arizona State University, Tempe, AZ 85287, USA.

³Department of Computer Science, IIITDharwad, Karnataka, 580009, India.

*Corresponding author. E-mail: a.josep52@asu.edu

Abstract

We present CosmicANNEstimator (Cosmological Parameters Artificial Neural Network Estimator), a machine learning approach for constraining cosmological parameters within the Lambda Cold Dark Matter (Λ CDM) framework. Our methodology employs two specialized artificial neural networks (ANNs) designed to analyze Hubble parameter and Supernova data independently. The estimator is trained on synthetic data covering broad parameter ranges, with Gaussian random noise incorporated to simulate observational uncertainties. Our results demonstrate parameter estimates and associated uncertainties comparable to traditional Markov Chain Monte Carlo (MCMC) methods, establishing machine learning as an efficient alternative for cosmological parameter estimation. This work underscores the potential of neural network-based inference to complement traditional Bayesian methods and accelerate future cosmological analyses.

Keywords: ANN, cosmological parameters, machine learning

1 Introduction

Modern cosmology has witnessed unprecedented advances over the past two decades, driven by a remarkable wealth of high-precision observational data. This wealth

of information has enabled rigorous testing and refinement of cosmological models, deepening our understanding of universal evolution. The Lambda Cold Dark Matter (Λ CDM) model has emerged as the predominant theoretical framework, emphasizing two fundamental components: cold dark matter, characterized by its slow-moving nature, and dark energy, a mysterious force that drives the accelerating expansion of the universe while opposing gravitational forces (Perlmutter et al. 1999; Spergel et al. 2007; Tegmark et al. 2004; Zhuravlev et al. 1998; Davis et al. 2007; Hicken et al. 2009; Hinshaw et al. 2009; Lima & Alcaniz 2000; Basilakos & Plionis 2010; Joseph & Saha 2021, 2022, 2023).

The quantification of cosmological parameters serves as a detailed blueprint of universal properties, providing crucial insights into cosmic evolution across temporal scales. These parameters form the essential bridge between theoretical frameworks and observational evidence, making their accurate estimation a fundamental pursuit in modern cosmology. The Markov Chain Monte Carlo (MCMC) method has traditionally been the cornerstone of parameter estimation, valued for its robust performance in both parameter value determination and uncertainty quantification. However, MCMC methodology faces significant challenges in the era of big data. As observational datasets grow in both volume and complexity, the computational demands of MCMC become increasingly prohibitive. The method's inherent requirement for numerous iterations to achieve proper convergence and thoroughly explore parameter space poses practical limitations for modern cosmological analyses. This computational bottleneck has spurred the search for more efficient analytical approaches. In response to these challenges, this work investigates an artificial intelligence-based solution for cosmological parameter estimation. While the use of ANNs for cosmological estimations is not novel, this work focuses on applying the ANN methodology to multiple datasets—specifically, Hubble data and supernova data.

Machine learning (ML) methods have revolutionized cosmological research in recent years, demonstrating exceptional performance in addressing complex challenges with both accuracy and efficiency (de Dios Rojas Olvera et al. 2022). The application of ML regression algorithms—including Artificial Neural Networks, KNN, Gradient Boosting, Extra-Trees and Support Vector Machines—has proven particularly effective in estimating H_0 and its associated uncertainties (Bengaly et al. 2023). Genetic Algorithms have emerged as a valuable complement to traditional MCMC methods, especially in constraining dark energy models such as Λ CDM, CPL, and PolyCPL (Medel-Esquivel et al. 2023).

Significant methodological advances have shaped the field's development. Auld et al. introduced COSMONET (Auld et al. 2007), a Bayesian inference algorithm that employs artificial neural networks (ANNs) to accelerate the calculation of Cosmic Microwave Background (CMB) likelihood functions and matter power spectra for estimating of cosmological parameter. Additionally, Graff et al. developed the blind accelerated multimodal Bayesian inference (BAMBI) algorithm (Graff et al. 2014), which combines nested sampling with ANNs for efficient likelihood function learning.

In the realm of Hubble parameter analysis, diverse analytical approaches have yielded valuable insights. Leaf and Melia (Leaf & Melia 2017) employed two-point statistics to evaluate cosmological models, focusing particularly on differential age

(DA) measurements of $H(z)$. Their work proved especially significant due to the model-independent nature of cosmic chronometer measurements. Extending this research, Geng et al. (Geng et al. 2018) combined DA and BAO (baryon acoustic oscillation) techniques to study $H(z)$ measurements, both for parameter determination and to assess the anticipated impact of next-generation $H(z)$ measurements on parameter estimation. Latest literature has increasingly focused on ML applications in low-redshift data analysis. Notable contributions by Arjona & Nesseris (Arjona & Nesseris 2020), Mukherjee et al. (Mukherjee et al. 2022), and Gómez-Valent & Amendola (Gómez-Valent & Amendola 2018) have successfully employed ML approaches to analyze Hubble measurements and Type Ia Supernovae observations to refine current cosmological parameter estimates.

The present work draws primary inspiration from two recent frameworks: EcoPANN (Wang et al. 2020) and ParamANN (Pal & Saha 2024). EcoPANN provides comprehensive estimation of cosmological parameters including H_0 , Ω_{bh^2} , Ω_{ch^2} , τ , $10^9 A_s$, and n_s , utilizing an innovative iterative approach to handle uncertainty in diverse cosmological datasets and predict joint constraints. ParamANN focuses on predicting the Hubble constant(H_0) and density parameters (Ω_{m0} , Ω_{k0} , Ω_Λ) of the Λ CDM model along with their uncertainties (σ_{H_0} , $\sigma_{\Omega_{m0}}$, $\sigma_{\Omega_{k0}}$, σ_{Ω_Λ}), employing Hubble measurements and a heteroscedastic loss function for uncertainty quantification.

This study aims to demonstrate the viability of ANNs with varying architectures as alternatives to traditional MCMC methods for cosmological parameter estimation. We employ heteroscedastic loss function to predict three fundamental cosmological parameters (H_0 , Ω_{m0} , and $\Omega_{\Lambda 0}$) using Hubble data. Also we extend this framework by developing an independent model trained specifically on Type Ia supernova data to predict two key parameters (Ω_{m0} , and $\Omega_{\Lambda 0}$), utilizing the same heteroscedastic uncertainty quantification approach. This dual-model strategy represents a significant departure from single-dataset approaches, enabling each model to extract and leverage distinct insights from its respective observational dataset.

1.1 Cosmological Dynamics

Cosmic evolutionary mechanisms are well understood within the framework of general relativity (GR) (Kinney 2003). The metric evolves according to the Einstein field equations, which relate the geometry of the spacetime with the matter content within it. The Einstein field equations which govern the dynamics of the Universe are given by (Kinney 2003),

$$G_{\mu\nu} \equiv R_{\mu\nu} - \frac{1}{2}g_{\mu\nu}R = 8\pi GT_{\mu\nu}, \quad (1)$$

where $G_{\mu\nu}$ is the Einstein tensor, G is the Newtonian gravitational constant, $R_{\mu\nu}$ is the Ricci tensor and R is the Ricci scalar. The geometry of spacetime is described by the left-hand side of the equation, while the energy-momentum content of the Universe is represented by the right-hand side through the energy-momentum tensor $T_{\mu\nu}$.

Using Eqn. 1, we can obtain Friedmann equations which govern dynamics of the universe given by,

$$\left(\frac{\dot{a}}{a}\right)^2 = \frac{8\pi G}{3}\rho - \frac{k}{a^2}, \quad (2)$$

$$\frac{\ddot{a}}{a} = -\frac{4\pi G}{3}(\rho + 3P). \quad (3)$$

In this context, ρ and P represent the aggregate energy density and pressure components in the universe. We denote ρ_m for the contribution by matter (with ρ_c for cold dark matter and ρ_b for baryons), and ρ_Λ signifies the vacuum energy contribution and ρ_r represents the contribution from radiation (with ρ_γ for photons and ρ_ν for neutrinos). The primary Friedmann equation is traditionally expressed via the Hubble parameter, $H \equiv \dot{a}/a$

$$H^2 = \frac{8\pi G}{3}\rho - \frac{k}{a^2}. \quad (4)$$

In the case of a flat universe ($k = 0$), the critical density of the Universe can be expressed as,

$$\rho_{\text{crit}0} = \frac{3H_0^2}{8\pi G}, \quad (5)$$

where the subscript ‘0’ denotes the present-epoch value of cosmological parameters.

The critical density serves as the reference point for expressing density parameters in dimensionless form:

$$\Omega_{I0} \equiv \frac{\rho_{I0}}{\rho_{\text{crit}0}}. \quad (6)$$

From this perspective, the Friedmann equation, (Eqn. 4) takes the following form

$$H^2(a) = H_0^2 \left[\Omega_{r0} \left(\frac{a_0}{a} \right)^4 + \Omega_{m0} \left(\frac{a_0}{a} \right)^3 + \Omega_{k0} \left(\frac{a_0}{a} \right)^2 + \Omega_{\Lambda0} \right], \quad (7)$$

where we have defined a curvature density parameter, $\Omega_{k0} \equiv -k/(a_0 H_0)^2$, H_0 is the present-day value of the Hubble parameter (the Hubble constant), Ω_{r0} denotes the present-day radiation density parameter for matter, Ω_{m0} denotes the present-day density parameter for matter and $\Omega_{\Lambda0}$ denotes the present-day density parameter for dark energy. By adopting the usual convention, we normalize the present-day scale factor to unity, $a_0 \equiv 1$. Eqn. 7 then becomes

$$\frac{H^2}{H_0^2} = \Omega_r a^{-4} + \Omega_m a^{-3} + \Omega_k a^{-2} + \Omega_\Lambda. \quad (8)$$

Using Eqn. 3, the Friedmann equation of the Λ CDM model in the late universe (we can neglect Ω_{r0}) with spatial curvature can be written as:

$$H^2(z) = H_0^2 \left[\Omega_{m0}(1+z)^3 + (1 - \Omega_{m0} - \Omega_{\Lambda0})(1+z)^2 + \Omega_{\Lambda0} \right] \quad (9)$$

where, $H(z)$ represents the Hubble parameter as a function of redshift. This equation 9 illustrates the mathematical model of Hubble parameters across different redshifts based on specific values of H_0 , Ω_{m0} , and $\Omega_{\Lambda0}$.

2 Methodology

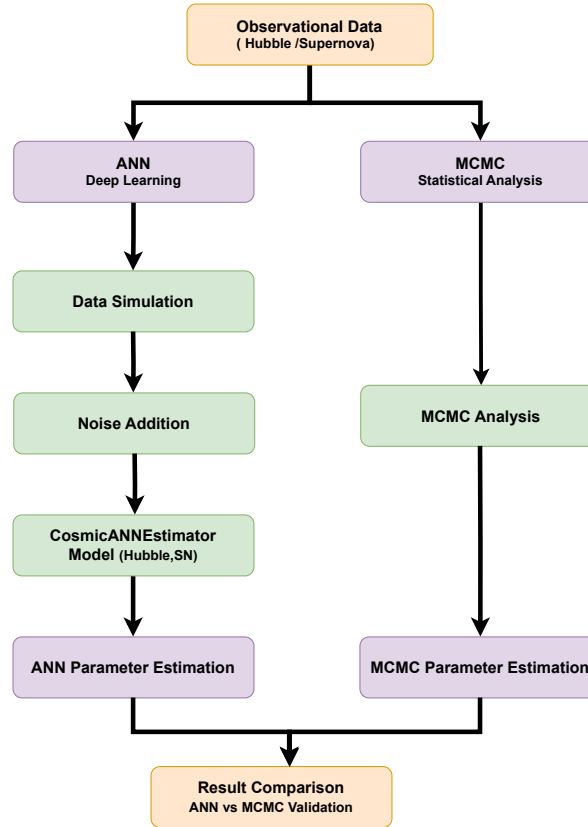


Fig. 1 Schematic representation of the CosmicANNEstimator framework integrating observational data processing, neural network training, and MCMC validation

Our study's methodological approach integrates four key components: First, we examine observational data obtained from Hubble measurements and Pantheon Type Ia Supernovae (SnIa). Second, we generate simulated values for the Hubble parameter $H(z)$ and luminosity distance $d_L(z)$, incorporating appropriate noise models. Third, we design and implement specialized neural network architectures for parameter estimation. Finally, we employ Markov Chain Monte Carlo (MCMC) analysis as a

validation framework to verify our results. Figure 1 shows the schematic representation of our approach.

2.1 Datasets

The datasets utilized in this work contain redshifts, an observable associated with each redshift and their respective statistical errors. Each redshift data point is accompanied by an associated observable—such as luminosity distance $d_L(z)$ or Hubble parameter $H(z)$ —and their respective statistical errors, which quantify the uncertainties in these measurements.

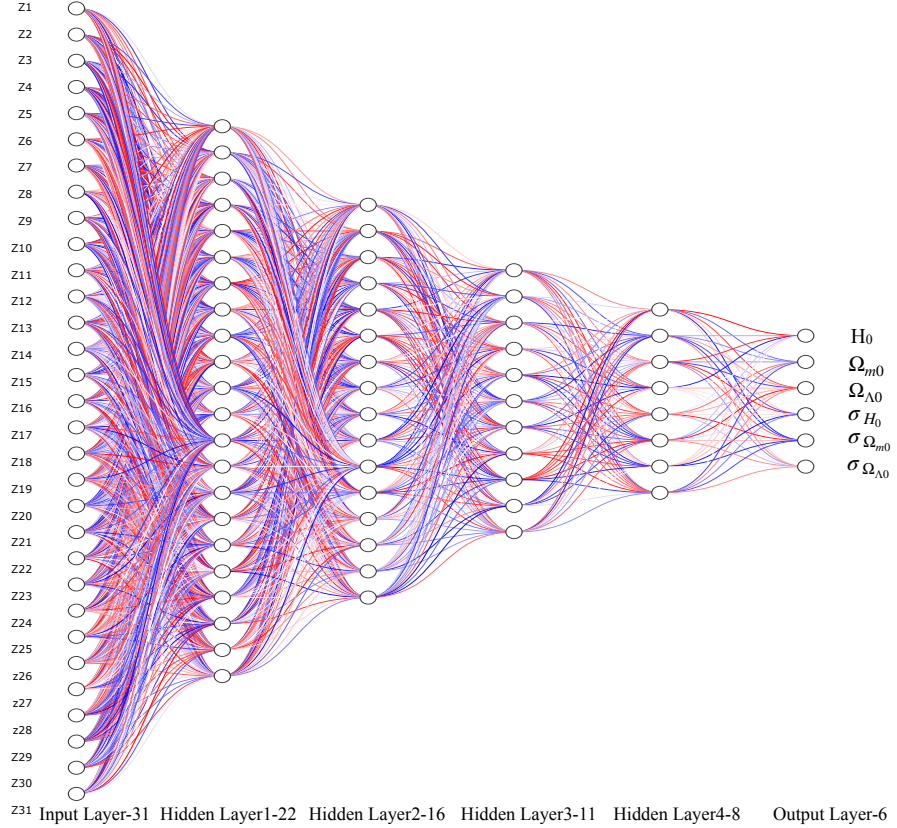


Fig. 2 The architecture of CosmicANNEstimator for Hubble Compilation. The network architecture consists of an input layer with 31 z -values, four hidden layers with 22, 16, 11, and 8 neurons respectively (with ReLU activation), and an output layer with 6 cosmological parameters.

2.1.1 $H(z)$ Compilation:

The Hubble parameter dataset comprises 31 measurements spanning a redshift range of $z \in [0.07, 1.965]$. These measurements were obtained using the Differential Age (DA) technique. Table 1 shows these measured $H(z)$ values and associated uncertainties expressed in $\text{km s}^{-1} \text{Mpc}^{-1}$ units (Jimenez & Loeb 2002).

2.1.2 Pantheon Supernova Dataset:

A total of 1,048 Type Ia Supernovae measurements are contained within the Pantheon sample in the redshift range $z \in [0.1, 2.26]$ (Perlmutter et al. 1999, 1997; Brout et al. 2022)

For both datasets, redshift points are arranged in ascending order to facilitate systematic generation of mock values for $H(z)$ and $d_L(z)$.

2.2 Data Simulations

2.2.1 $H(z)$ Compilation:

A uniform distribution is considered in the range $\{50, 90\} \text{ km Mpc}^{-1} \text{ sec}^{-1}$ for H_0 , the range $\{0.1, 0.7\}$ for Ω_{m0} , and the range $\{0.3, 0.9\}$ for $\Omega_{\Lambda 0}$. Using the numpy library's `random.uniform` function, we generate 120,000 random samples for each parameter, ensuring comprehensive coverage of the parameter space.

For each parameter set, we compute the Hubble parameter $H(z)$ at 31 observed redshift points using Eqn. 9. This process yields 120,000 distinct realizations of $H(z)$ measurements across the observed redshift range.

2.2.2 Pantheon Supernova Dataset:

The Eqn. 9 can be rewritten as

$$H(z) = H_0 \sqrt{\Omega_m(1+z)^3 + \Omega_\Lambda}, \quad (10)$$

here H_0 is fixed at $66.99 \text{ km s}^{-1} \text{ Mpc}^{-1}$

The luminosity distance $d_L(z)$ is defined as:

$$d_L(z) = (1+z) \int_0^z \frac{cdz'}{H(z')}, \quad (11)$$

where c is the speed of light. The angular diameter distance $d_A(z)$ can be calculated using the cosmic distance duality relation:

$$d_A(z) = \frac{d_L(z)}{(1+z)^2}. \quad (12)$$

For Type Ia Supernovae (SNe Ia), the distance modulus $\mu(z)$ is given by:

$$\mu(z) = 5 \log_{10} \left(\frac{d_L(z)}{\text{Mpc}} \right) + 25. \quad (13)$$

The numerical integration required for $d_L(z)$ is performed using Simpson's 1/3 method, generating 120,000 realizations of $\mu(z)$ at 1048 observed redshift points.

Table 1 Hubble parameter measurements $H(z)$ and respective uncertainties, $\sigma(H(z))$ at different redshifts z (Jimenez & Loeb 2002).

z	$H(z)$	$\sigma(H(z))$
0.07	69	19.6
0.09	69	12
0.12	68.6	26.2
0.17	83	8
0.1791	75	4
0.1993	75	5
0.2	72.9	29.6
0.27	77	14
0.28	88.8	36.64
0.3519	83	14
0.3802	83	13.5
0.4	95	17
0.4004	77	10.2
0.4247	87.1	11.2
0.4497	92.8	12.9
0.47	89	34
0.4783	80.9	9
0.48	97	62
0.5929	104	13
0.6797	92	8
0.7812	105	12
0.8754	125	17
0.88	90	40
0.9	117	23
1.0375	154	20
1.3	168	17
1.363	160	33.6
1.43	177	18
1.53	140	14
1.75	202	40
1.965	186.5	50.4

2.3 Adding Noise to Data

In supervised learning applications, training data should accurately reflect the statistical properties of test data—in this case, observational measurements. Each measurement X is assumed to follow a Gaussian distribution $N(X, \sigma^2)$, where X represents the mean value and σ denotes associated measurement uncertainty. Yet, the values generated by the theoretical model do not have errors. Thus, before training the artificial neural network (ANN), the simulated data should be adjusted to match the spread of the observational data. We simulate observational uncertainties by adding Gaussian random noise to the synthetic datasets.

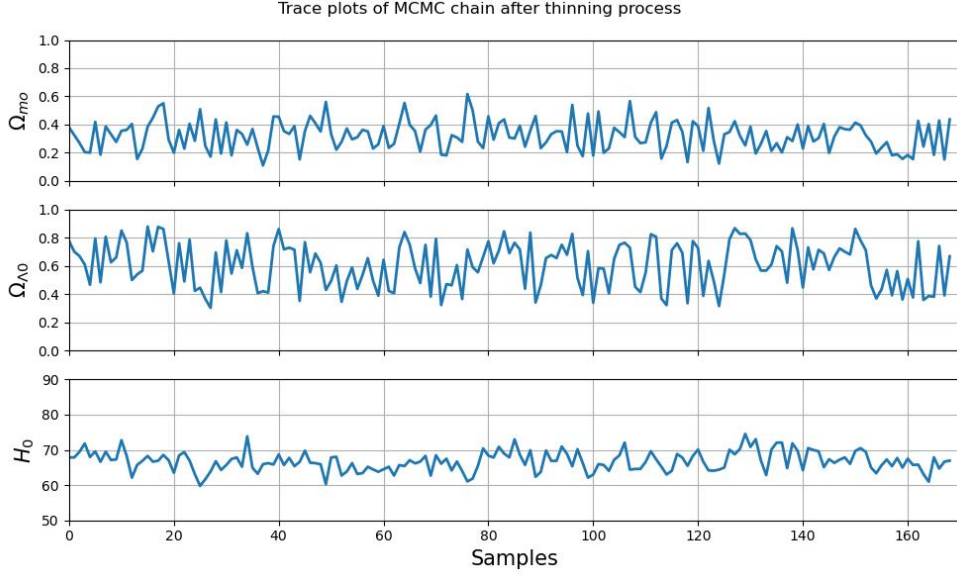


Fig. 3 Figure showing trace plots of Hubble Parameter Data after performing thinning process

To achieve this, we incorporate random noise following Gaussian probability density to the simulated data, aligning it with the error level of the observational measurements used for cosmological parameter estimation. This adjustment helps to prevent distribution inconsistency, overfitting, and enhances the generalization of the trained model. For each measurement, random deviates are drawn from a normal distribution $N(X, \sigma^2)$, where σ corresponds to the observed uncertainty at each redshift point, using the `random.normal` function. This random number is then added to both $H(z)$ and $\mu(z)$ corresponding to the data set.

2.4 Data Preprocessing

The complete dataset is partitioned into three distinct subsets: a training set, a validation set, and a testing set. 10^5 data points are allocated for training, 1.5×10^4 data points are allocated for validation, and 5×10^3 data points for testing the CosmicanNEstimator predictions. This partitioning ensures robust model training, proper validation for hyperparameter optimization, and unbiased performance evaluation.

2.4.1 Data Preprocessing for the Hubble Compilation:

For the Hubble parameter compilation, we implement a standardization procedure to optimize neural network training. We first compute two key statistical parameters from the noise-integrated measurements $H(z)$ in our training dataset: the average value and its statistical spread (standard deviation). We then perform data standardization across all datasets (training, validation, and testing) using these computed parameters.

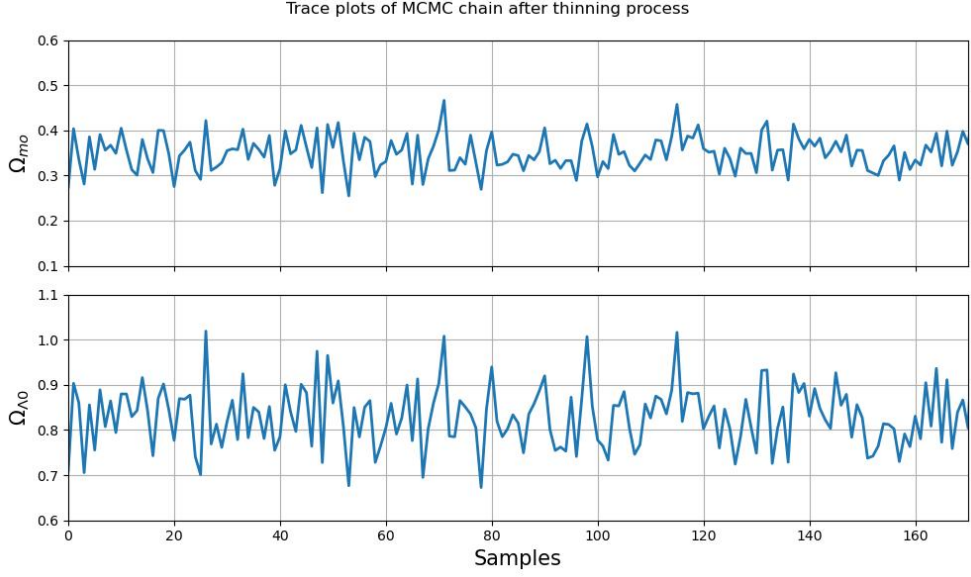


Fig. 4 Figure showing trace plots of Supernova Data after performing thinning process

We normalize each data by subtracting this average value and dividing by the standard deviation calculated from the training set. After this preprocessing, the standardized data is used for training the ANN.

2.5 Proposed Model

The core of our methodology centers on a sophisticated deep learning approach designed specifically for cosmological parameter estimation. We implement an artificial neural network (ANN) architecture that processes measurements through a series of carefully designed transformations to predict fundamental cosmological parameters and their associated uncertainties.

Our parameter estimation framework employs a feed-forward neural network that systematically transforms observational data into cosmological parameter estimates. The network processes information through multiple stages, each implementing specific transformations designed to capture the complex relationships inherent in cosmological data. Observational measurements first enter the network through a dedicated input layer, where they undergo initial processing. These processed signals then propagate through multiple hidden layers, where non-linear transformations extract and refine relevant features from the data. Finally, a specialized output layer generates both parameter estimates and their corresponding uncertainties, providing a complete statistical description of the cosmological parameters of interest.

2.5.1 Proposed Model for Hubble Compilation - CosmicANNEstimator-Hubble:

For the analysis of Hubble parameter measurements, we implement a carefully optimized network architecture comprising six distinct layers. The input layer contains 31 neurons, corresponding to the dimensionality of the Hubble parameter dataset. This is followed by four hidden layers implementing Rectified Linear Unit (ReLU) activation functions, with 22, 16, 11 and 8 neurons respectively. The ReLU activation function, expressed mathematically as $f(x) = \max(0, x)$, enables efficient network training while maintaining the capacity to capture non-linear relationships in the data. The architecture culminates in an output layer of 6 neurons, where the first three neurons generate direct parameter estimates for H_0 , Ω_{m0} , $\Omega_{\Lambda0}$, while the remaining three neurons provide their corresponding uncertainty estimates. The network implements full connectivity between successive layers, ensuring comprehensive parameter space exploration through dense connections. For network optimization, we implement the Adaptive Moment Estimation (ADAM) algorithm, which combines the advantages of both adaptive gradient algorithms and momentum methods. The training process employs a carefully tuned learning rate of 5×10^{-4} , determined through extensive experimentation to ensure stable convergence while maintaining efficient parameter updates during backpropagation. This optimization strategy allows the network to effectively navigate the parameter space while avoiding local minima and ensuring robust convergence to optimal weight and bias values. The combination of noise-integrated training data, non-linear activation functions, and sophisticated optimization techniques enables our network to develop a robust understanding of the relationship between observational data and cosmological parameters. The training process continues until convergence criteria are met. Figure 2 presents the architecture of CosmicANNEstimator for Hubble Compilation.

2.5.2 Proposed Model for Pantheon Supernova Dataset - CosmicANNEstimator-SN:

The implementation of CosmicANNEstimator for Type Ia supernova analysis employs a distinct architectural approach from the Hubble parameter estimation network. For supernova analysis, we focus exclusively on determining the density parameters (Ω_{m0} , $\Omega_{\Lambda0}$) of the Λ CDM model, working directly with uncalibrated supernova data without standardization preprocessing.

The supernova analysis network implements a deep architecture optimized for the high-dimensional nature of the Pantheon dataset. The input layer comprises 1048 neurons, corresponding to the dimensionality of the observational data. This is followed by a cascade of five hidden layers with progressively decreasing neuron counts: 512, 256, 128, 64, and 32 neurons, respectively with ReLU activation function. This pyramidal structure enables systematic feature extraction and dimensionality reduction while maintaining essential cosmological information. Full connectivity is maintained between successive layers to ensure comprehensive information flow through the network.

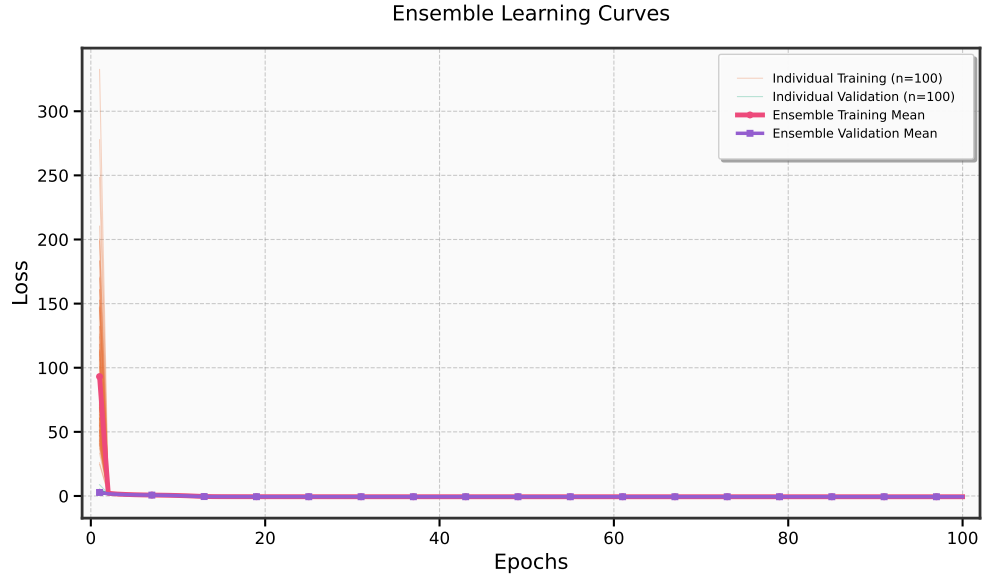


Fig. 5 Figure showing Learning Curve of CosmicANNEstimator-Hubble Model

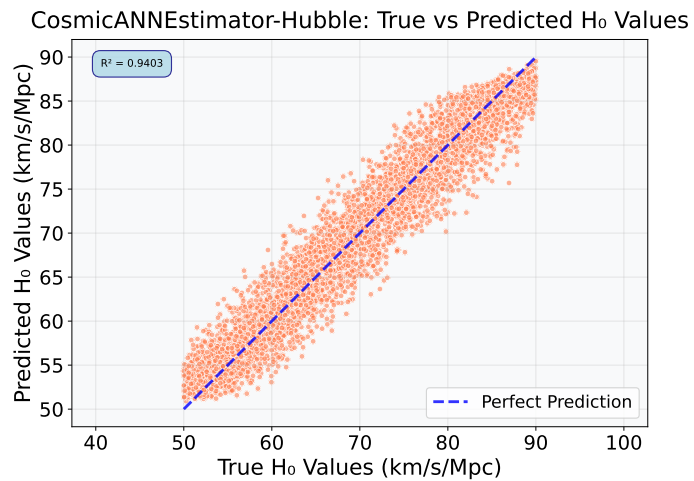


Fig. 6 Figure showing Performance Evaluation of True vs Predicted values for Hubble Constant (H_0) for CosmicANNEstimator-Hubble. Coefficient of determination, $R^2 = 0.9403$, shows strong agreement between predicted and true H_0 values

The network culminates in an output layer containing four neurons: two dedicated to parameter estimation (Ω_{m0} and $\Omega_{\Lambda0}$) and two for their associated uncertainties. This design differs from the Hubble parameter estimation network by excluding H_0 prediction.

Network training implements specific hyperparameters optimized for the supernova analysis task. We employ a batch size of 128 samples, which balances computational efficiency with stable gradient estimates. The training proceeds for 200 epochs, allowing sufficient time for convergence while avoiding overfitting. A learning rate of 1×10^{-5} is implemented, enabling fine-grained weight adjustments necessary for the precise parameter estimation required in cosmological applications.

2.6 Loss function

Our methodology implements a heteroscedastic (HS) (Kendall & Gal 2017) loss function for uncertainty quantification in parameter estimation. The function is defined as:

$$L_{HS} = \frac{1}{2n} \sum_{q=1}^n \exp(-s_a) (y_a - \hat{y}_a)^2 + s_a \quad (14)$$

where n specifies the number of actual values. In the equation, y_a and \hat{y}_a represent the predictions and actual values respectively. Additionally, log variances ($\ln \sigma_a^2$) corresponding to the predictions is represented by s_a , where σ_a specifies the aleatoric uncertainty of the prediction. By implementing this specific loss function design, we can determine the predictive uncertainty (aleatoric) associated with each individual output.

The output layer architecture of CosmicANNEstimator varies based on the dataset used. For Hubble Compilations, the output layer contains six neurons: three neurons estimate the cosmological parameters ($H_0, \Omega_{m0}, \Omega_{\Lambda0}$), while the other three calculate their corresponding uncertainties. In contrast, when processing the Pantheon Supernova Dataset, the output layer consists of four neurons: two neurons predict the cosmological density parameters ($\Omega_{m0}, \Omega_{\Lambda0}$), and the remaining two neurons compute their respective uncertainties.

The heteroscedastic loss function shares fundamental similarities with negative log-likelihood functions commonly employed in traditional MCMC-based cosmological parameter estimation. However, the optimization methodologies differ substantially. Traditional Bayesian approaches minimize noise variance through likelihood functions, typically assuming Gaussian distributions, to extract optimal parameter values from observational data. In contrast, our neural network implementation represents a likelihood-evaluation-free inference method (Alsing et al. 2018), where the loss function quantifies the discrepancy between predicted and reference values based on training data. Despite these methodological differences, comparative analysis demonstrates that both approaches yield consistent results when applied to both Hubble measurements and Pantheon Supernova data, validating the robustness of our neural network methodology.

2.7 Model Training

The CosmicANNEstimator adopts an ensemble learning strategy encompassing 100 independent training realizations with standardized hyperparameter configurations. Each training realization employs a validation set containing 1.5×10^4 data points

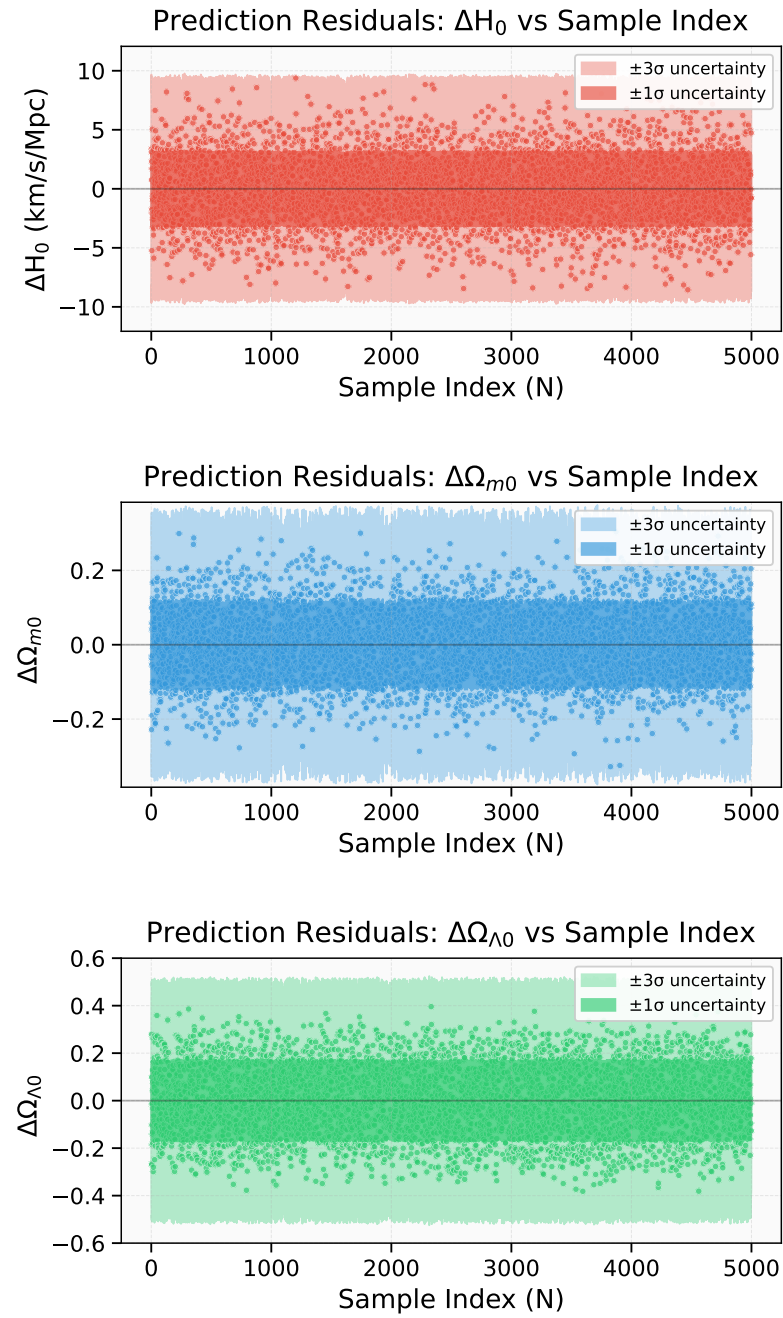


Fig. 7 Figure showing distribution of differences between model outputs and true values of the Hubble constant, matter density and dark energy density parameters across various realizations (N) of the test set

for performance optimization. These 100 trained models are subsequently employed for cosmological parameter estimation from observational datasets.

The training process demonstrates robust convergence characteristics, with no evidence of overfitting or underfitting across the ensemble. The complete training procedure for the 100-member ensemble for CosmicANNEstimator-Hubble model required approximately 180 minutes of computation time on an AMD64 Family 25 Model 80 CPU system (8 cores, 16 threads, 3.2 GHz processor).

2.8 Model prediction on Simulated Data

The parameter estimation procedure utilizes a test set containing 5×10^4 data points, evaluated across the 100-member ensemble of trained models. Each of the 100 ensemble model generates both parameter estimates and log-variances through the heteroscedastic loss function.

Final parameter estimates are computed as the mean of predictions across all ensemble members for each test realization. Uncertainty calculations follow a systematic two-step process: first, log-variances from each ensemble member are exponentiated to obtain individual variances, then averaged across the 100 members. Final uncertainties are derived by taking the square root of these averaged variances.

The residuals between predicted and actual values are evaluated to verify that parameter differentials predominantly remain within three times the predicted uncertainty ($\pm 3\sigma$) bounds, thereby confirming robust agreement between predictions and reference values and validating the model's ability to provide estimates with accurate uncertainty quantification across the parameter space.

2.9 MCMC

We implement the Metropolis-Hastings algorithm (Hastings 1970) to sample posterior distributions of three cosmological parameters (H_0 , Ω_{m0} , and $\Omega_{\Lambda0}$), utilizing identical prior ranges as the CosmicANNEstimator method. The likelihood function for the data is defined as:

$$\mathcal{L}_{data}(\theta) = e^{-\chi_{data}^2(\theta)/2} \quad (15)$$

where χ_{data}^2 denotes Hubble data or Supernova data based on the dataset and θ represents the model's variable parameters. The optimal parameter values (θ) are determined by identifying those that yield the lowest possible χ^2 value.

We employed MCMC sampling to identify high-confidence regions for our model parameters, constrained by the observational dataset. Through likelihood analysis, we minimized the χ^2 function (Eq. 15), leading to the determination of optimal model parameters at the χ^2 minimum.

We initiated our MCMC analysis using a conventional proposal function: $\theta_{i+1}^j = \theta_i^j + \delta\theta^j \eta^j$ where j denotes the parameter index, $\delta\theta^j$ represents the predefined rms step size, and η^j is a Gaussian stochastic variate with zero mean and unit variance. Given that our model incorporates three parameters with strong intercorrelations,

this basic approach proved suboptimal. Therefore, we implemented several optimization techniques on the MCMC chain samples to enhance both the acceptance ratio and chain convergence. Following the generation of a preliminary chain with sufficient samples, we evaluated the chain's autocorrelation. This analysis provided crucial insights into determining the necessary number of Markov chain iterations required for effectively independent samples. Subsequently, we applied thinning to the initial chain to reduce sample correlations, thereby decreasing the overall sample size while maintaining statistical validity.

From the resulting samples, we calculate the covariance matrix: $C_{ij} = \langle \delta\theta^i \delta\theta^j \rangle$

We then apply Cholesky decomposition to this matrix: $\mathbf{C} = \mathbf{L}\mathbf{L}^t$ where \mathbf{C} represents the covariance matrix, \mathbf{L} denotes the lower triangular matrix, and \mathbf{L}^t is its conjugate transpose. Using these results, we reformulate our proposal function as: $\theta_{i+1} = \theta_i + \alpha \mathbf{L}\boldsymbol{\eta}$ Here, $\boldsymbol{\eta}$ represents a vector of Gaussian variates, and α is an overall scale factor, initially set to approximately 0.3. This reformulation ensures that proposed samples exhibit the appropriate covariance structure, substantially improving sampling efficiency. To maintain optimal sampling performance, we implement bounds on the acceptance ratio, requiring it to fall between 5% and 80%. The scale factor α can be adjusted when these bounds are exceeded, preventing either excessively large or small step sizes.

Trace plot analysis presented in Figures 3 and 4, offers additional confirmation of proper chain convergence through post-thinning visualization of parameter evolution. The Hubble parameter trace plots exhibit stable random fluctuations around mean values for all three parameters ($H_0, \Omega_{m0}, \Omega_{\Lambda0}$), while the supernova analysis demonstrates similar stability for its two parameters ($\Omega_{m0}, \Omega_{\Lambda0}$). In both cases, the trace plots show no evidence of systematic trends or long-term drifts, displaying instead consistent oscillation patterns that indicate proper exploration of the parameter space. The absence of chain sticking or extreme parameter excursions, combined with uniform exploration around central values, provides strong evidence for reliable posterior sampling in both analyses.

2.9.1 Convergence test:

The goal of MCMC sampling is to draw samples from a target distribution, ideally reaching a point where samples are representative of this distribution. However, MCMC chains can take time to converge, especially if initialized in different regions of the parameter space. The Gelman-Rubin diagnostic provides a quantitative way to evaluate whether the chains have "mixed" well enough and converged to the target distribution, ensuring that further sampling will yield reliable estimates. The statistical relationships can be written mathematically as:

$$E = \frac{1}{M(N-1)} \sum_{i=1}^M \sum_{j=1}^N (\Theta_{ij} - \bar{\Theta}_i)^2 \quad (16)$$

$$F = \frac{N}{M-1} \sum_{i=1}^M (\bar{\Theta}_i - \bar{\Theta})^2 \quad (17)$$

$$G = (1 - \frac{1}{N})E + \frac{1}{N}F \quad (18)$$

In these equations, the variable M indicates the total chain count, while N signifies the number of data points within each individual chain. We evaluate the MCMC algorithm's convergence using the R statistic developed by Gelman and Rubin, $R = V/W$, which should approach unity for proper convergence. Our analysis yields R-values of 0.9996 and 0.995 for the Hubble parameter and supernova data analyses, respectively, indicating excellent convergence.

3 Results and Analysis

We evaluate two distinct implementations of CosmicANNEstimator: one optimized for Hubble measurements(CosmicANNEstimator-Hubble) and another designed for Type Ia Supernova (SnIa) observations(CosmicANNEstimator-SN). Each variant undergoes testing with its corresponding dataset—the Hubble-based model with Hubble parameter measurements and the Supernova-based model with Pantheon Supernova observations. The models' predictions are validated against estimations from dedicated MCMC analyses for their respective datasets.

3.1 Predictions for Hubble Compilation using CosmicANNEstimator-Hubble

3.1.1 Predictions on Test Set:

The learning dynamics of the Hubble parameter model demonstrate robust convergence characteristics, as illustrated in Figure 5. The ensemble training (red curve) and validation (purple curve) losses demonstrate convergence within the first 10-12 epochs, maintaining minimal separation throughout the 100-epoch training period. The ensemble means for both training and validation losses remain consistently low and closely aligned, indicating optimal model generalization without overfitting across all 100 ensemble members.

We evaluate the model's accuracy by testing it against $H(z)$ measurements from our reserved test dataset to estimate the Hubble constant (H_0), matter density (Ω_{m0}), and dark energy density ($\Omega_{\Lambda0}$). Figure 6 demonstrates the correlation between predicted and actual Hubble constant values, revealing a strong linear relationship that confirms the model's estimation accuracy.

Parameter prediction accuracy is quantified through the deviation metric:

$$\Delta y = \hat{y} - y$$

where y denotes the model predictions and \hat{y} represents the reference (true) values.

Figure 7 presents a comprehensive analysis of parameter prediction residuals across the test set of 5000 samples. The three panels display the deviations for the Hubble

constant ΔH_0 (top), matter density parameter $\Delta\Omega_{m0}$ (middle), and dark energy density parameter $\Delta\Omega_{\Lambda0}$ (bottom). Each panel includes shaded bands representing one and three times the predicted uncertainty ($\pm 1\sigma$ and $\pm 3\sigma$) for the respective parameters. The analysis reveals that parameter residuals are predominantly contained within the $\pm 3\sigma$ uncertainty bounds, with the vast majority falling within the $\pm 1\sigma$ bands, demonstrating excellent agreement between model predictions and reference values. The distribution of residuals across all parameters exhibits symmetric behavior around zero. This confirms the model's ability to deliver accurate predictions with reliable uncertainty quantification.

3.1.2 Predictions On Observational Data:

The CosmicANNEstimator, trained on simulated $H(z)$ values incorporating observational noise patterns, processes standardized observed $H(z)$ measurements to extract cosmological parameters and their uncertainties. A parallel MCMC analysis as mentioned in Section 2.9 provides independent parameter estimations using identical observational data, enabling direct comparison of both methodologies.

Our analysis yields consistent parameter estimates across both methods for three fundamental cosmological parameters:

Table 2 Comparison of parameter values H_0 (in $\text{km s}^{-1} \text{Mpc}^{-1}$), Ω_{m0} , and $\Omega_{\Lambda0}$ estimated by MCMC and CosmicANNEstimator for Hubble data (Jimenez & Loeb 2002).

Parameter	MCMC	CosmicANNEstimator
H_0	66.99 ± 2.99	67.14 ± 3.12
Ω_{m0}	0.321 ± 0.104	0.317 ± 0.109
$\Omega_{\Lambda0}$	0.620 ± 0.154	0.621 ± 0.165

The uncertainties are expressed as $\pm 1\sigma$.

The comparative analysis reveals strong concordance between both methods across all three fundamental cosmological parameters as mentioned in Table 2. For the Hubble constant (H_0), CosmicANNEstimator yields $H_0 = 67.1448 \pm 3.122 \text{ km s}^{-1} \text{ Mpc}^{-1}$, closely matching the MCMC estimate of $H_0 = 66.9943 \pm 2.9918 \text{ km s}^{-1} \text{ Mpc}^{-1}$. The matter density parameter (Ω_{m0}) shows similar agreement, with CosmicANNEstimator producing $\Omega_{m0} = 0.3174 \pm 0.1087$ compared to the MCMC value of $\Omega_{m0} = 0.3213 \pm 0.1038$. For the dark energy density parameter ($\Omega_{\Lambda0}$), CosmicANNEstimator estimates $\Omega_{\Lambda0} = 0.6209 \pm 0.1654$, in strong agreement with the MCMC result of $\Omega_{\Lambda0} = 0.6204 \pm 0.1537$.

The MCMC posterior distributions, illustrated in Figure 8 through a corner plot, provide deeper insight into parameter relationships. The marginalized distributions show peaks consistent with our point estimates: $67-68 \text{ km Mpc}^{-1} \text{ sec}^{-1}$, $\Omega_{\Lambda0}$ centered near 0.6, and Ω_{m0} approximately at 0.3. The two-dimensional joint distributions,

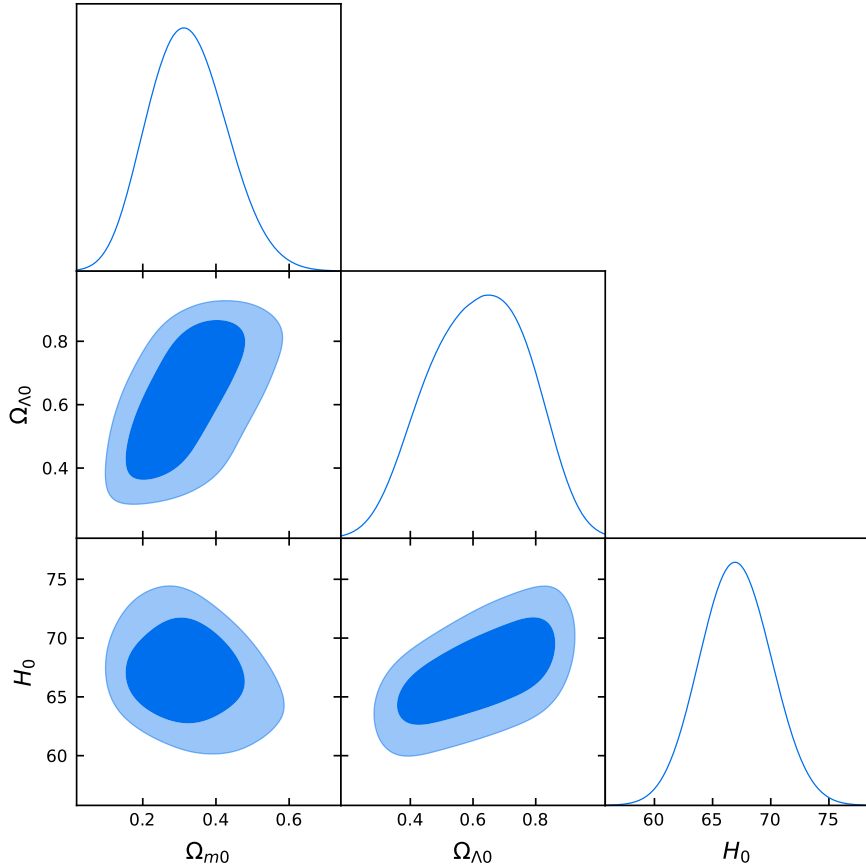


Fig. 8 Figure showing MCMC posterior distributions for cosmological parameters for Hubble dataset

depicted with 68% (dark blue) and 95% (light blue) confidence contours, reveal the correlations between parameters and confirm the robustness of our estimates.

The consistency between CosmicANNEstimator and MCMC results, both in parameter values and their associated uncertainties, validates the effectiveness of our neural network approach for cosmological parameter estimation of Hubble Observations.

3.2 Predictions for Pantheon Supernova Dataset using CosmicANNEstimator-SN

3.2.1 Predictions on Test Set:

The CosmicANNEstimator's predictive capabilities for Type Ia Supernovae data are evaluated using noise-incorporated $d_L(z)$ measurements from the test dataset. The model demonstrates robust performance in estimating both matter density (Ω_{m0}) and

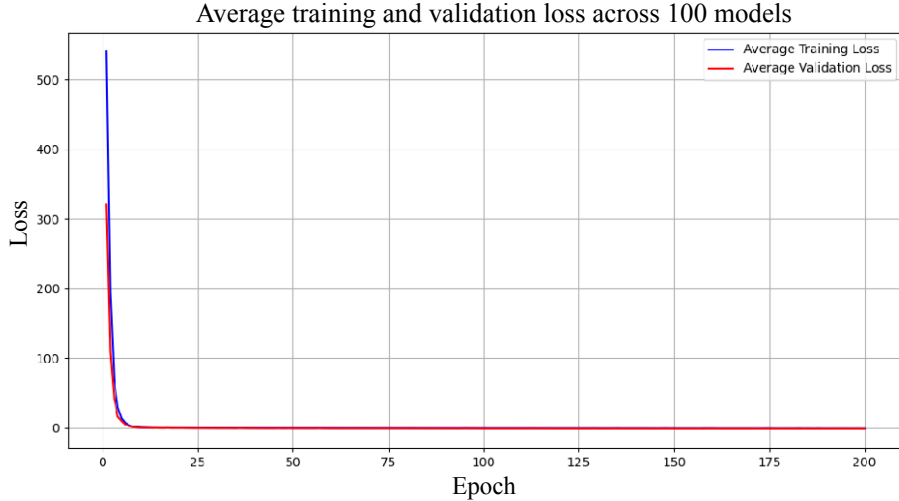


Fig. 9 Figure showing learning curve of CosmicANNEstimator-SN Model

dark energy density ($\Omega_{\Lambda 0}$) parameters, with predictions exhibiting strong alignment with target values.

Analysis of the training dynamics reveals learning behavior across epochs, as shown in Figure 9. At the beginning (around epoch 0 to 20), there is a significant drop in both training and validation loss, indicating that the model quickly learns patterns in the data in the early epochs. After around epoch 20, both the training and validation loss values stabilize at a much lower value, and the decrease in loss becomes minimal for the remainder of the training. The average training loss (in blue) and validation loss (in red) closely follow each other throughout the epochs, with minimal divergence. This suggests that the model has a good fit and is not overfitting, as there isn't a large gap between training and validation losses.

3.2.2 Predictions On Observational Data:

The CosmicANNEstimator for Type Ia supernova analysis employs simulated luminosity distance measurements that incorporate uncertainties matching the observed Pantheon dataset characteristics. We process observed luminosity distance values through the trained model to estimate two fundamental cosmological parameters: matter density (Ω_{m0}) and dark energy density ($\Omega_{\Lambda 0}$), along with their associated uncertainties. A parallel MCMC analysis following methodology detailed in Section 2.9 provides independent parameter estimations using identical Pantheon supernova measurements. Table 3 presents the comprehensive comparison between both approaches.

For the matter density parameter (Ω_{m0}), MCMC yields a value of 0.35006 ± 0.04002 , while the CosmicANNEstimator estimates 0.2830 ± 0.0588 . For the dark energy density parameter $\Omega_{\Lambda0}$, MCMC calculates 0.8308 ± 0.0677 , compared to CosmicANNEstimator's estimation of 0.9025 ± 0.1089 . Although the best-fit values of parameters (Ω_{m0} and $\Omega_{\Lambda0}$) from supernova datasets deviate slightly from their MCMC values, they are consistent at 1-sigma with their corresponding MCMC results. It is also interesting to note that the ANN method produces larger uncertainties compared to MCMC.

Table 3 Comparison of parameter values Ω_{m0} and $\Omega_{\Lambda0}$ estimated by MCMC and CosmicANNEstimator for Supernova data.

Parameter	MCMC	CosmicANNEstimator
Ω_{m0}	0.35006 ± 0.04002	0.2830 ± 0.0588
$\Omega_{\Lambda0}$	0.8308 ± 0.0677	0.9025 ± 0.1089

The uncertainties are expressed as $\pm 1\sigma$.

The figure 10 illustrates the MCMC posterior distributions for cosmological parameters derived from Type Ia Supernova data analysis. The plot is structured as a corner plot showing both marginalized and joint distributions for matter density (Ω_{m0}) and dark energy density ($\Omega_{\Lambda0}$) parameters. The diagonal panels display one-dimensional marginalized posterior distributions, with Ω_{m0} centered approximately at 0.35 and $\Omega_{\Lambda0}$ peaking around 0.83. The off-diagonal panel reveals the two-dimensional joint distribution with confidence intervals represented by dark blue (68%) and light blue (95%) contours. The narrow width of the posterior distributions suggests well-constrained parameter estimates from the Supernova data.

Using Hubble parameter data we obtain the present value of Hubble Constant, $H_0 = 67.1448 \pm 3.122 \text{ km s}^{-1} \text{ Mpc}^{-1}$, demonstrating remarkable agreement with the latest Planck 2018 measurements (Planck Collaboration et al. 2020).

4 Effect of Hyperparameters

Neural network performance is inherently sensitive to architectural and training configuration choices. While default hyperparameter values were established in the preceding analysis Section 2.5, systematic investigation of their impact on parameter estimation accuracy is essential for optimal model design. This section presents a comprehensive sensitivity analysis examining how hyperparameters—including network depth, activation function selection and learning rate influence on the results for Hubble CosmicANNEstimator model.

To evaluate the influence of model design and training choices on predictive performance, we define a significance metric to quantify deviations from benchmark results. For each cosmological parameter $\theta \in \{H_0, \Omega_{m0}, \Omega_{\Lambda0}\}$ the neural network provides both a mean prediction and an associated uncertainty (σ).

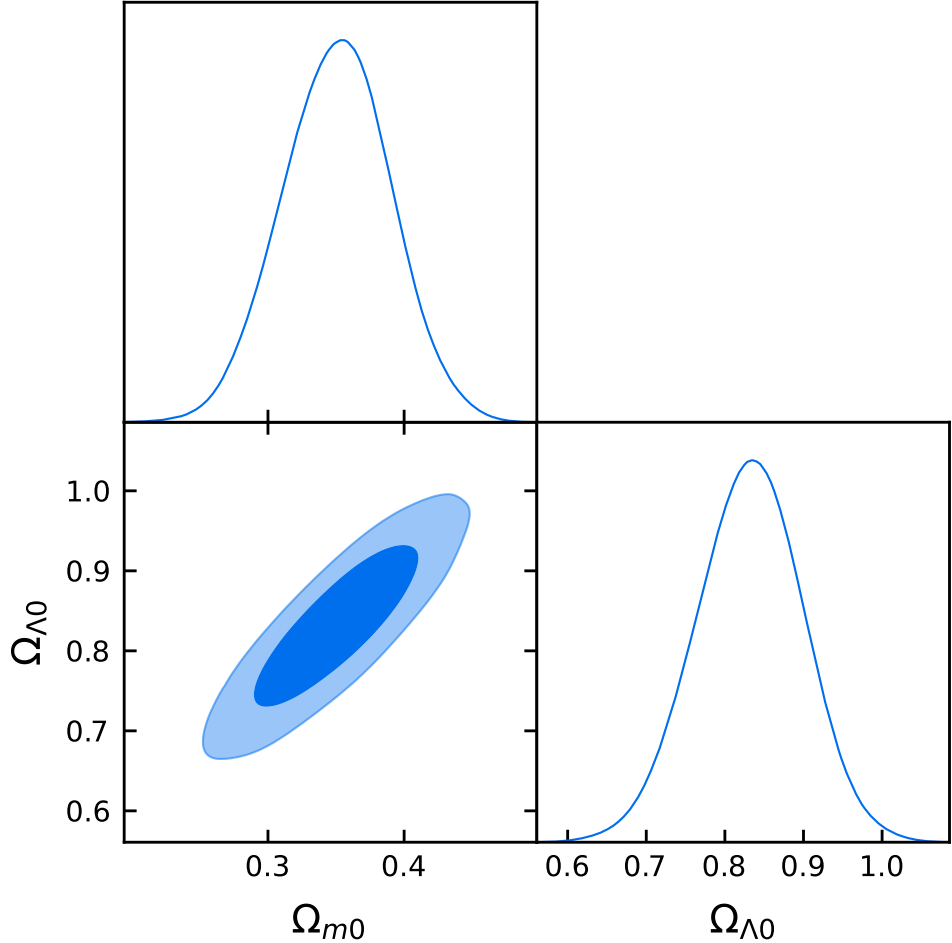


Fig. 10 Figure showing MCMC posterior distributions for cosmological parameters for Supernova Dataset

The absolute deviation between ANN predictions and MCMC reference values is calculated as:

$$\Delta\theta = |\theta^{\text{ANN}} - \theta^{\text{MCMC}}| \quad (19)$$

This deviation is then normalized by the model's predicted uncertainty:

$$\delta\theta = \frac{\Delta\theta}{\sigma_\theta} \quad (20)$$

which expresses how many standard deviations the ANN prediction lies away from the MCMC benchmark. The overall significance is defined as the sum of the relative deviations across all parameters:

Effect Of Hyperparameters

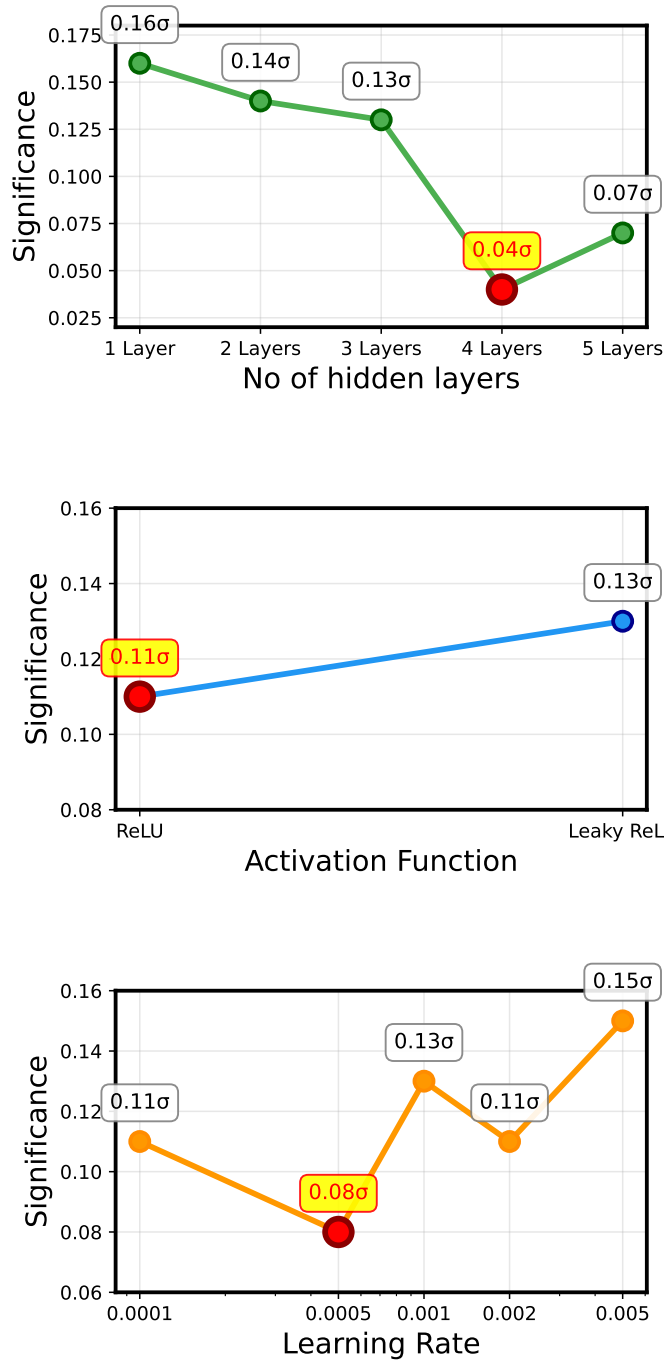


Fig. 11 Figure showing hyperparameter sensitivity analysis for CosmicANNEstimator-Hubble with significance levels of ANN-MCMC deviations

$$S = \delta H_0 + \delta \Omega_{m0} + \delta \Omega_{\Lambda 0} \quad (21)$$

This metric serves as a consolidated measure of how closely the ANN predictions align with MCMC results, with lower significance values indicating stronger overall consistency across all cosmological parameters.

4.1 The Number of Hidden Layers

We first test the effect of the number of hidden layers in the ANN model. We design five different ANN structures with the number of hidden layers from 1 to 5, where the number of neurons in each layer is set according to Equation (22).

$$N_i = \left\lfloor \frac{N_{\text{in}}}{F^i} \right\rfloor, \quad i = 1, 2, \dots, n_{\text{layers}} \quad (22)$$

The decreasing factor F is calculated as:

$$F = \left(\frac{N_{\text{in}}}{N_{\text{out}}} \right)^{\frac{1}{n_{\text{layers}}+1}} \quad (23)$$

where:

- N_{in} is the number of input neurons
- N_{out} is the number of output neurons
- n_{layers} is the number of hidden layers

where $\lfloor \cdot \rfloor$ denotes the floor function to ensure integer neuron counts.

In addition, the activation function is ReLU, and the learning rate is 0.0005. Then, five sets of ANNs are trained, and the parameters are predicted using these models according to the procedure in [Section 2.7](#). Furthermore, we calculate significance of deviations between ANN and MCMC results (Equation 20). The significance as a function of the number of hidden layers is shown in the top panel of Figure 11, where the maximum deviation is 0.16σ (for the ANN with one hidden layer) and the minimum deviation is 0.04σ (for the ANN with four hidden layers).

Starting with a single hidden layer, the network exhibits moderate performance with a significance of 0.16σ . This relatively high deviation suggests that a shallow architecture lacks sufficient representational capacity to capture the complex non-linear relationships inherent in cosmological parameter estimation. As the network depth increases to 2 layers, performance improves marginally to 0.14σ , followed by a further enhancement at 3 layers (0.13σ). This gradual improvement indicates that additional layers initially provide beneficial feature abstraction capabilities, allowing the network to learn hierarchical representations of the input cosmological data. The most significant performance gain occurs at 4 hidden layers, where the significance drops to 0.04σ . This represents the optimal architecture depth, achieving excellent agreement with MCMC benchmark results. The substantial improvement suggests that 4 layers provide the ideal balance between model complexity and generalization capability, enabling effective extraction of cosmological parameter relationships without overfitting. However, further increasing the depth to 5 layers results in performance

degradation, with significance rising to 0.07σ . Therefore, we adopt the ANN structure that has four hidden layers in our analysis.

4.2 Activation Function

To test the effect of activation function on the results of parameter estimations, we select two kinds of rectified units: rectified linear (ReLU) and leaky rectified linear (LeakyReLU).

The ReLU activation function is defined as:

$$f(x) = \begin{cases} x & \text{if } x > 0 \\ 0 & \text{if } x \leq 0 \end{cases} \quad (24)$$

ReLU can introduce non-linearity while maintaining gradient flow for positive inputs. The leaky ReLU is defined as:

$$f(x) = \begin{cases} x & \text{if } x > 0 \\ \alpha x & \text{if } x \leq 0 \end{cases} \quad (25)$$

where α is a small positive constant, we set α to be 0.01 in our analysis.

Leaky ReLU is designed to address the “dying ReLU” problem by allowing small negative gradients.

In our analysis, the structure of the ANN with four hidden layers is adopted, and the learning rate is 0.0005. With the same procedure as [Section 2.7](#), we estimate cosmological parameters with ANNs by adopting these two different activation functions. After obtaining parameters, the mean deviations of parameters between the ANN results and MCMC values are calculated along with the significance, shown in the central panel of [Figure 11](#). The standard ReLU function demonstrates superior performance with a significance of 0.11σ , outperforming Leaky ReLU which achieves 0.13σ . Therefore, the ReLU activation function is used in this work.

4.3 Learning Rate

The learning rate analysis, depicted in the bottom panel of [Figure 11](#), reveals strong sensitivity to this hyperparameter across five different values ranging from 1×10^{-4} to 5×10^{-3} .

At the lowest learning rate of 1×10^{-4} , the model achieves moderate performance with a significance of 0.11σ . The modest performance suggests that while training stability is maintained, the optimization process may not effectively explore the parameter space to find optimal network weights. The optimal performance occurs at a learning rate of 5×10^{-4} , yielding the lowest significance of 0.08σ . This intermediate value appears to strike the ideal balance between training stability and convergence efficiency. The learning rate is sufficiently large to enable effective gradient descent while remaining small enough to prevent overshooting optimal solutions. As the learning rate increases to 1×10^{-3} , performance degrades significantly to 0.13σ . Further increases to

2×10^{-3} and 5×10^{-3} result in continued deterioration, with significances of 0.11σ and 0.15σ respectively.

4.4 Effect of hyper parameters on CosmicANNEstimator-SN

A similar hyperparameter optimization study was conducted for the supernova model architecture, following the same systematic approach employed for the Hubble Model analysis. The investigation revealed that a 5-layer neural network configuration with ReLU activation functions provided optimal performance for supernova parameter estimation tasks. Notably, the supernova model required a more conservative learning rate of 1×10^{-5} , an order of magnitude lower than the Hubble model’s optimal rate of 5×10^{-4} . This reduced learning rate was essential to prevent instabilities during training while maintaining convergence to parameter estimates.

5 Conclusion

We have developed a comprehensive methodology for cosmological parameter estimation using artificial neural networks through the CosmicANNEstimator framework. Our approach implements two specialized architectures: CosmicANNEstimator-Hubble and CosmicANNEstimator-SN, each specifically designed and optimized for analyzing Hubble parameter measurements and Type Ia Supernova datasets, respectively. The framework’s training implementation utilized 10^5 mock samples of $H(z)$ and $d_L(z)$ values, incorporating realistic noise characteristics that match observational data properties. The models employ distinct prior ranges tailored to their respective datasets: CosmicANNEstimator-Hubble uses $H_0 \in \{50, 90\}$ km Mpc $^{-1}$ s $^{-1}$, $\Omega_{m0} \in \{0.1, 0.7\}$, and $\Omega_{\Lambda0} \in \{0.3, 0.9\}$, while CosmicANNEstimator-SN employs $\Omega_{m0} \in \{0, 1\}$ and $\Omega_{\Lambda0} \in \{0, 1.5\}$.

CosmicANNEstimator-Hubble features a six-layer architecture with an input layer of 31 neurons, four hidden layers with ReLU activation functions (22, 16, 11, and 8 neurons respectively), and an output layer predicting six parameters (H_0 , Ω_{m0} , $\Omega_{\Lambda0}$) with their associated uncertainties. CosmicANNEstimator-SN employs a deeper seven-layer architecture, beginning with 1048 input neurons corresponding to observational data points, followed by five hidden layers with progressively decreasing neuron counts (512, 256, 128, 64, and 32 neurons), concluding with an output layer predicting two parameters (Ω_{m0} , $\Omega_{\Lambda0}$) and their uncertainties. Both models underwent rigorous validation using 1.5×10^4 mock data samples and comprehensive testing with 5×10^3 samples. Testing results demonstrate that differences between target values and predictions consistently fall within three standard deviations of the predicted uncertainties.

The trained models were successfully applied to real observational datasets. CosmicANNEstimator-Hubble analyzed 31 observed Hubble parameter measurements spanning redshift range $0.07 \leq z \leq 1.965$, yielding $H_0 = 67.1448 \pm 3.122$ km Mpc $^{-1}$ s $^{-1}$, $\Omega_{m0} = 0.3174 \pm 0.1087$, and $\Omega_{\Lambda0} = 0.6209 \pm 0.1654$. CosmicANNEstimator-SN processed 1048 Type Ia Supernova data points, producing $\Omega_{m0} = 0.2830 \pm 0.0588$ and $\Omega_{\Lambda0} = 0.9025 \pm 0.1089$. The CosmicANNEstimator-Hubble model demonstrates

results consistent with traditional MCMC methods, while the best-fit values predicted by CosmicANNEstimator-SN deviate slightly from their MCMC values. Both models provide substantial computational advantages.

We summarize the findings and advantages of our method as follows:

1. Unlike MCMC approaches requiring explicit likelihood functions, these neural network-based methods learn parameter relationships directly from training data, providing particular utility for complex, high-dimensional astronomical datasets where likelihood function specification becomes challenging.
2. The complete training procedure for the 100-member ensemble of CosmicANNEstimator-Hubble required approximately 180 minutes on an AMD64 Family 25 Model 80 CPU system (8 cores, 16 threads, 3.2 GHz processor). Similarly, the CosmicANNEstimator-SN training procedure required approximately 240 minutes on the same computational setup. Following the training phase, parameter estimation for new datasets is achieved with negligible computational overhead for both models, representing a substantial improvement over MCMC methods which typically require significant computational resources and extended runtime for each new analysis. Parameter estimation for the Hubble dataset containing 31 observational points required approximately 20 seconds of computation time, while the Supernova dataset comprising 1048 data points processed through CosmicANNEstimator-SN completed parameter inference within approximately 40 seconds.
3. Our neural network approach demonstrates a favorable computational profile, with resource allocation primarily concentrated in two phases: initial training set generation and network training. The efficiency of the ANN approach becomes particularly relevant in the context of modern astronomical surveys, where data volumes continue to expand. While the initial investment in training time is non-negligible, the subsequent rapid parameter estimation capabilities provide a compelling advantage for large-scale cosmological analyses. This computational efficiency positions neural network methodologies as particularly valuable tools for current and future astronomical surveys where rapid analysis of extensive datasets is essential.
4. In this work, we describe our framework as a likelihood-evaluation-free inference method, since the inference stage avoids explicit likelihood evaluations or statistical sampling that are central to traditional Bayesian or MCMC approaches. Instead, the ANN provides parameter estimates and uncertainties through a predictive ML-based mapping learned from simulations generated under the Λ CDM model. This differs from fully simulation-based inference (SBI) frameworks ([Papamakarios & Murray 2016](#); [Cranmer et al. 2020](#)), which can treat the forward model as a true black box, whereas our approach remains anchored to analytic cosmological equations for simulation generation. The ML approaches uncover direct mapping between input and targets to learn hidden patterns between them, providing a complementary mechanism to traditional likelihood-based methods for testing the robustness of scientific results.

5. The CosmicANNEstimator models demonstrate excellent predictive performance within training boundaries. Extrapolation beyond these limits yields poor performance, confirming that reliable parameter estimation is restricted to the training parameter space.
6. Our CosmicANNEstimator, like most deep neural networks, functions as a black box where the internal decision-making is not directly interpretable. While MCMC follows explicit likelihood-based reasoning that can be traced, the ANN learns complex non-linear mappings between data and parameters without clear physical interpretation. In this work, we focused on demonstrating numerical consistency with MCMC and computational efficiency, while improving interpretability—through feature attribution methods or physics-informed architectures—remains an important direction for future development
7. Our study identifies several key advantages of ANN-based parameter estimation over traditional MCMC approaches in cosmological contexts. The ability of neural networks to perform parameter inference with minimal computational requirements establishes them as exceptionally suitable tools for large-scale cosmological studies requiring rapid analysis of multiple datasets.
 - Modern and upcoming astronomical surveys (such as LSST ([Ivezić et al. 2019](#)), Euclid ([Euclid Collaboration et al. 2025](#)), and Roman Space Telescope ([Wenzl et al. 2022](#))) will generate unprecedented volumes of data requiring rapid analysis. ANN framework can process thousands of datasets in the time required for a single MCMC analysis, making it ideal for survey forecasts, systematic studies across parameter spaces, and batch processing of observational catalogs.
 - The instantaneous nature of ANN prediction enables real-time cosmological parameter estimation from new observations. This capability is particularly valuable for time-critical applications, adaptive observing strategies, and interactive analysis workflows where immediate feedback is essential.
 - While MCMC requires substantial computational resources for each individual analysis, ANN approach front-loads the computational investment during training, then provides essentially cost-free inference thereafter. This amortization of computational cost becomes increasingly advantageous as the number of analyses grows, making ANNs particularly cost-effective for large-scale cosmological studies.

To summarize, the advantages of ANN approach, Neural network method is particularly advantageous when: (1)analyzing large volumes of data from modern astronomical surveys; (2)requiring rapid parameter estimation for multiple datasets; (3)working with high-dimensional observational data where likelihood function specification becomes challenging; (4)conducting survey forecasts requiring analysis of thousands of simulated datasets; (5)implementing real-time or interactive analysis workflows; and (6)performing systematic studies across large parameter spaces where computational efficiency is paramount.

A significant limitation of our current approach is the absence of full parameter covariance information. The heteroscedastic loss function provides only diagonal uncertainty estimates and cannot capture parameter correlations such as the well-known

H_0 - Ω_{m0} degeneracy. This represents an important area for future development, potentially through approaches such as Cholesky decomposition of covariance matrices or normalizing flow-based posterior modeling.

Also, as a future extension of this work, the CosmicANNEstimator framework could be expanded to perform joint analysis of Type Ia Supernova (SN Ia) and Hubble datasets. This enhanced approach would potentially improve the precision of parameter constraints for the Λ CDM model.

References

Perlmutter, S., Aldering, G., Goldhaber, G., et al. 1999, *Astroph. J.* , 517, 2, 565. doi:10.1086/307221

Spergel, D. N., Bean, R., Doré, O., et al. 2007, *ApJS*, 170, 2, 377. doi:10.1086/513700

Tegmark, M., Strauss, M. A., Blanton, M. R., et al. 2004, *Phys. Rev. D* , 69, 10, 103501. doi:10.1103/PhysRevD.69.103501

Basilakos, S. & Plionis, M. 2010, *Astroph. J. Lett.*, 714, L185. doi:10.1088/2041-8205/714/2/L185

Davis, T. M., Mörtsell, E., Sollerman, J., et al. 2007, *Astroph. J.* , 666, 716. doi:10.1086/519988

Hicken, M., Wood-Vasey, W. M., Blondin, S., et al. 2009, *Astroph. J.* , 700, 1097. doi:10.1088/0004-637X/700/2/1097

Hinshaw, G., Weiland, J. L., Hill, R. S., et al. 2009, *ApJS*, 180, 225. doi:10.1088/0067-0049/180/2/225

Lima, J. A. S. & Alcaniz, J. S. 2000, *Mon. Not. Roy. Ast. Soc.* , 317, 893. doi:10.1046/j.1365-8711.2000.03695.x

Zhuravlev, V. M., Chervon, S. V., & Shchigolev, V. K. 1998, *Soviet Journal of Experimental and Theoretical Physics*, 87, 2, 223. doi:10.1134/1.558649

Joseph, A. & Saha, R. 2021, *Journal of Astrophysics and Astronomy*, 42, 2, 111. doi:10.1007/s12036-021-09776-6

Joseph, A. & Saha, R. 2022, *Mon. Not. Roy. Ast. Soc.* , 511, 2, 1637. doi:10.1093/mnras/stac201

Joseph, A. & Saha, R. 2023, *Mon. Not. Roy. Ast. Soc.* , 519, 2, 1809. doi:10.1093/mnras/stac3586

de Dios Rojas Olvera, J., Gómez-Vargas, I., & Vázquez, J. A. 2022, *Universe*, 8, 2, 120. doi:10.3390/universe8020120

Bengaly, C., Dantas, M. A., Casarini, L., et al. 2023, European Physical Journal C, 83, 6, 548. doi:10.1140/epjc/s10052-023-11734-1

Medel-Esquivel, R., Gómez-Vargas, I., Morales Sánchez, A. A., et al. 2023, Universe, 10, 1, 11. doi:10.3390/universe10010011

Auld, T., Bridges, M., Hobson, M. P., et al. 2007, Mon. Not. Roy. Ast. Soc. , 376, 1, L11. doi:10.1111/j.1745-3933.2006.00276.x

Graff, P., Feroz, F., Hobson, M. P., et al. 2014, Mon. Not. Roy. Ast. Soc. , 441, 2, 1741. doi:10.1093/mnras/stu642

Leaf, K. & Melia, F. 2017, Mon. Not. Roy. Ast. Soc. , 470, 2, 2320. doi:10.1093/mnras/stx1437

Geng, J.-J., Guo, R.-Y., Wang, A.-Z., et al. 2018, Communications in Theoretical Physics, 70, 4, 445. doi:10.1088/0253-6102/70/4/445

Arjona, R. & Nesseris, S. 2020, Phys. Rev. D , 101, 12, 123525. doi:10.1103/PhysRevD.101.123525

Mukherjee, P., Said, J. L., & Mifsud, J. 2022, JCAP, 2022, 12, 029. doi:10.1088/1475-7516/2022/12/029

Gómez-Valent, A. & Amendola, L. 2018, JCAP, 2018, 4, 051. doi:10.1088/1475-7516/2018/04/051

Wang, G.-J., Li, S.-Y., & Xia, J.-Q. 2020, ApJS, 249, 2, 25. doi:10.3847/1538-4365/aba190

Pal, S. & Saha, R. 2024, PhyS, 99, 11, 115007. doi:10.1088/1402-4896/ad804d

Kinney, W. H. 2003, arXiv e-prints , astro-ph/0301448. doi:10.48550/arXiv.astro-ph/0301448

Jimenez, R. & Loeb, A. 2002, Astroph. J. , 573, 1, 37. doi:10.1086/340549

Perlmutter, S., Aldering, G., Deustua, S., et al. 1997, AJ, 191, 85.04. doi:10.48550/arXiv.astro-ph/9812473

Brout, D., Scolnic, D., Popovic, B., et al. 2022, Astroph. J. , 938, 2, 110. doi:10.3847/1538-4357/ac8e04

Kendall, A. & Gal, Y. 2017, , arXiv:1703.04977. doi:10.48550/arXiv.1703.04977

Alsing, J., Wandelt, B., & Feeney, S. 2018, Mon. Not. Roy. Ast. Soc. , 477, 3, 2874. doi:10.1093/mnras/sty819

Hastings W. K. 1970, Monte Carlo sampling methods using Markov chains and their applications, *Biometrika*, 57, 97

Planck Collaboration, Aghanim, N., Akrami, Y., et al. 2020, *AAp*, 641, A6.
doi:10.1051/0004-6361/201833910

Papamakarios, G. & Murray, I. 2016, , arXiv:1605.06376.
doi:10.48550/arXiv.1605.06376

Cranmer, K., Brehmer, J., & Louppe, G. 2020, *Proceedings of the National Academy of Science*, 117, 48, 30055. doi:10.1073/pnas.1912789117

Ivezić, Ž., Kahn, S. M., Tyson, J. A., et al. 2019, *Astroph. J.* , 873, 2, 111.
doi:10.3847/1538-4357/ab042c

Euclid Collaboration, Mellier, Y., Abdurro'uf, et al. 2025, *AAp*, 697, A1.
doi:10.1051/0004-6361/202450810

Wenzl, L., Doux, C., Heinrich, C., et al. 2022, *Mon. Not. Roy. Ast. Soc.* , 512, 4, 5311.
doi:10.1093/mnras/stac790